Macromolecular Research, Vol. 22, No. 1, pp 67-73 (2014)
DOI 10.1007/s13233-014-2013-1

www.springer.com/13233
pISSN 1598-5032 eISSN 2092-7673

Enhancement of Barrier Property of Plastic Substrate by Intra-Gallery Polymerization for Nanocomposites

You Jung Park[1], Hyun Gi Kim[1], Eun Hye Kim[2], and Sung Soo Kim*[,1,2]

[1]Department of Chemical Engineering, Kyung Hee University, Gyeonggi 446-701, Korea
[2]Regional Innovation Center for Components and Materials for Information Display, Kyung Hee University, Gyeonggi 446-701, Korea

Received June 10, 2013; Revised September 3, 2013; Accepted September 3, 2013

Abstract. 2-(Methacryloyloxy)ethyl(4-benzoylbenzyl) dimethyl ammonium bromide (MDAB) was successfully synthesized and used as a photo initiator and intercalation agent to induce intra-gallery polymerization. MDAB effectively replaced the sodium ions in the inter-gallery layer of sodium montmorillonite (Na^+-MMT) by the cationic exchange reaction, which was confirmed by inductively coupled plasma atomic emission spectroscopy (ICP-AES). The modification of Na^+-MMT with MDAB increased the *d*-spacing, with the MDAB/Na^+-MMT ratio of 2:1 doubling the initial *d*-spacing. Clay with modified MDAB was used to make a nanocomposite layer formation on a poly(ethylene naphthalate) (PEN) substrate by the photopolymerization of bisphenol A type epoxy diacrylate (EpA). Intra-gallery polymerization using MDAB attained more effective intercalation and better dispersion of the clay than extra-gallery polymerization using commercial organoclay. The clay content affected the barrier properties, and the best result was obtained at 5 wt% clay content, producing a water vapor transmission rate (WVTR) of 0.39 g/m^2 day while maintaining the optical transmittance.

Keywords: nanocomposite, intra-gallery polymerization, barrier property, plastic substrate.

Introduction

Barrier properties are essential for the plastic substrate in order to prevent the damages to liquid crystals and organic light emitting materials by moisture and oxygen through the substrate.[1] Various methods to make barrier layers have been developed such as inorganic layer deposition, organic layer coating and multilayer formation method by their combination.[2] Inorganic layers are formed by deposition processes such as chemical vapor deposition, sputtering and atomic layer deposition, and have achieved quite high barrier properties. However, most of the deposition processes should be performed at high vacuum and elevated temperature, which caused high cost and long process time. Inorganic deposition process has limitations to be applied to the roll-to-roll process. Moreover, inorganic deposition layers have brittle nature to cause handling problems and defect formation.

Organic layers are formed by solution coating followed by curing process to increase the density of layer. Organic layers have free volume inside and it could not attain the satisfactory barrier properties. Incorporation of inorganic filler to make composite layer was proposed to enhance the mechanical and barrier properties. Composite layer formation has many advantages such as simple coating process at ambient temperature and pressure. It can be performed by roll-to-roll process and costs much less than inorganic layer deposition process.

Since Toyota's central research laboratory developed Nylon/clay composites by monomer immersion in the clay galleries to enhance mechanical property and thermal stability in 1987,[3] the study of clay/polymer composites has been extensively investigated.[4] The research group in Cornell University reported polystyrene/clay composite layer by using polymer melting polymerization.[5] Giannelis studied intercalated structure and exfoliated structure of polymer/nanocomposites for analysis of its mechanism.[6] Many reports showed that polymer/nanocomposites are effective for improvement of mechanical property,[7] thermal stability,[8] and barrier properties.[9] Recently, UV curable polymer/clay composites has been studied for eco-friendly, fast curable, energy reducible process. Zahouily's research group investigated UV curable urethane/clay nanocomposites to confirm the exfoliated clays by X-ray diffraction.[10] Subramani *et al.* induced silylation for mechanically and thermally enhanced polyurethane/clay composites without increase of inter-layer spacing of clay.[11]

Recently, organic-inorganic multi layer formation is proposed for Al_2O_3 inorganic layer by reactive sputtering and acrylate based organic layer to have 10^{-6} g/m^{2}day of WVTR

*Corresponding Author. E-mail: sungkim@khu.ac.kr

value for OLED application.[12] Multilayer, however, has the adhesive degradation between coating layers' interface due to repeated process of sputter and UV curing. For these disadvantages, the research of composite layer was actively conducted.

Polymer composites reinforced using clays have many advantages, such as possibility to roll-to-roll process, low cost, and no process at vacuum and high temperature.[13] Sodium montmorillonite (Na^+-MMT) have been widely used as inorganic clay material. Therefore, in order to increase affinity with polymer, they should be organically modified. Several research groups have studied about clay modification.[14] Inter-layer spacing, however, was hard to increase just with intercalation agent due to practically existent monomer and photo-initiator in the clay galleries.

In this work, MDAB was synthesized for its use as an intercalation agent as well as a photo-initiator. MDAB is expected to replace the sodium ions of Na^+-MMT to achieve intercalation of clay and to induce the intra-gallery polymerization. Intra-gallery polymerization is investigated in terms of intercalation and exfoliation of clay during the polymerization, and is compared with the conventional extra-gallery polymerization. Performance enhancement of the composite layers formed by intra-gallery polymerization will be examined.

Experimental

Materials. Na^+-MMT with cationic exchange capacity (CEC) of 90 mEq/100 g was supplied by Southern Clay Product Co., USA. Nanomer 1.28E, which was organically modified by quaternary trimethyl stearyl ammonium, with CEC of 140 mEq/100 g was supplied by Nanocor Inc., USA. 4-bromomethyl benzophenone (BMBP, Aldrich Co.) and dimethyl-aminoethyl-methacrylate (DMAEMA, Aldrich Co.) were used to synthesize cationic photo initiator, 2-(methacryloyloxy) ethyl (4-benzoylbenzyl) dimethyl ammonium bromide (MDAB) and 1-hydroxy-cyclohexyl-phenyl-ketone (HCPK, Shin Young Radchem. Co., Korea) was used as a photo initiator.

Bisphenol A type epoxy diacrylate (EpA, Kukdo Chemical Co.) was used as a oligomer, and hexanediol diacrylate (HDDA, Miwon Specialty Chem., Korea.) and trimethylolpropane triacrylate (TMPTA, Miwon Specialty Chem., Korea.) were used as reactive diluents for oligomer. *N*,*N*-Dimethylformamide (DMF, Daejung Chemicals and Metals Co., Korea.) and methyl alcohol (Daejung Chemicals and Metals Co., Korea.) were used as solvent for coating solution. Poly(ethylene naphthalate) (PEN) (Q65) substrate of 0.2 mm of thickness was provided by Teijin DuPont Films, Japan.

Characterizations. The chemical analyses were performed by using Nuclear magnetic resonance (NMR) at 300 MHz (JNM-AL300, JEOL Ltd., Japan) and Fourier transformed infrared (FTIR) (System 2,000, Perkin Elmer Co., USA). The X-ray diffraction (XRD) patterns were obtained by using an X-ray diffractometer (D8 Advance, Bruker Co., USA) equipped with a CuK_α tube and Ni filter (k=0.1542 nm). The residual cation contents of clay were determined by an inductively coupled plasma atomic emission spectroscopy (ICP-AES) (Optima-4300 DV, Perkin Elmer Co., USA). The barrier property of coating layer was characterized by measuring water vapor transmission rate (WVTR) by using Permatran-W model 3/33, Mocon Inc., USA. The light transmittance of the sample was measured using a color filter spectral multi channel spectrophotometer (MCPD-3000 of Otsuka Co., Japan). Haze was determined using a NDH 5000, Nippon Denshoku Co. Japan. The final morphology of coating layer was observed by using field emission transmission electron microscope (FE-TEM) (JEM-2100F model, JEOL Ltd., Japan).

Results and Discussion

MDAB Synthesis and Clay Modification. MDAB, which is a multi-role surfactant working as an intercalating agent as well as a photo initiator, was synthesized with 5 g of BMBP and 4.67 g of DMAEMA in 300 mL of acetone at 55 °C for 8 h according to the reaction scheme as shown in Figure 1.[15] Synthesis of MDAB was confirmed by ^{1}H NMR as shown in Figure 2. Synthesized MDAB was repeatedly centrifuged and rinsed with distilled water for removal of the unreacted monomers, and then dried in vacuum oven overnight.

Na^+-MMT was modified by MDAB by cationic exchange reaction according to the mechanism as represented in Fig-

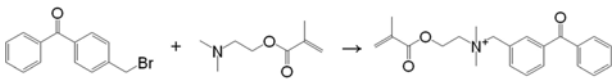

Figure 1. Reaction scheme for MDAB synthesis.

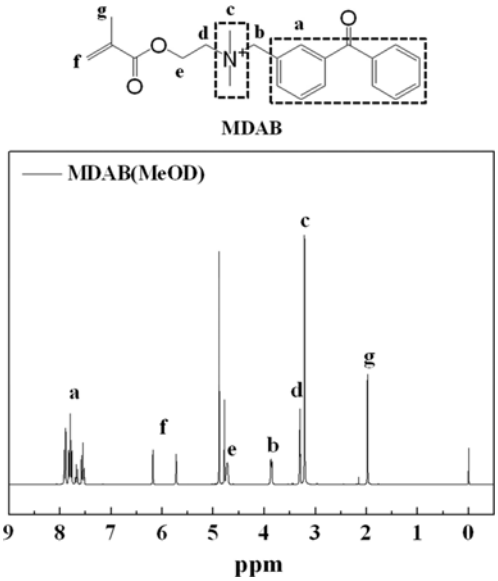

Figure 2. ^{1}H NMR spectra of synthesized MDAB.

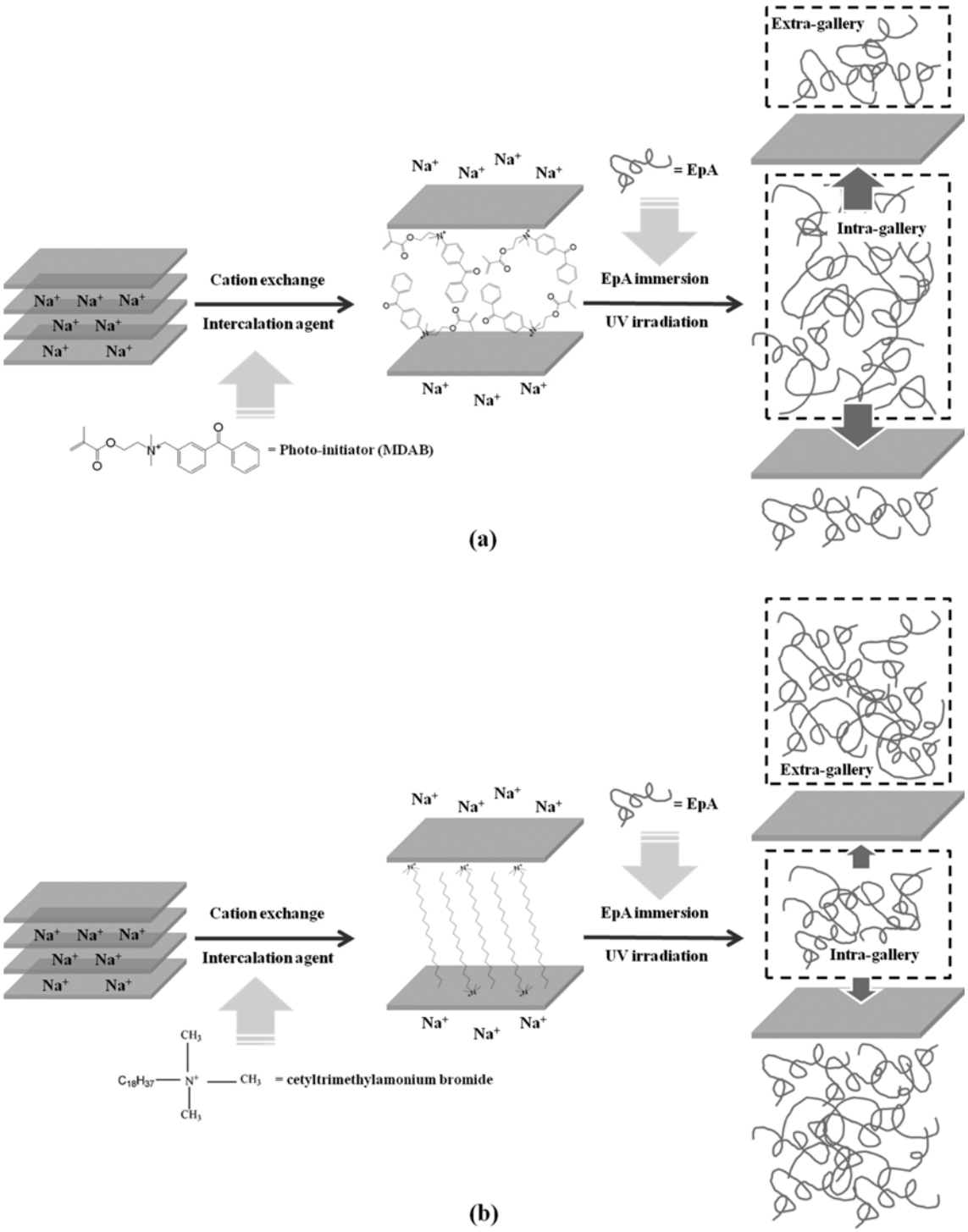

Figure 3. Mechanism scheme of photopolymerization of EpA. (a) Intra-gallery polymerization and (b) extra-gallery polymerization.

ure 3(a). 2 g of Na^+-MMT was dispersed in distilled water-methanol solution (5:6 by volume ratio) for 6 h and the clay solution was treated by probe-type ultra-sonicator for 5 min at room temperature. MDAB solution, 4 g of MDAB in 60 mL of water-methanol solution, was added by drop into clay solution followed by stirring for 6 h at 60 °C. Modified clay was washed and centrifuged repeatedly with distilled water for removal of unreacted monomers, and then dried in vacuum oven overnight.

Clay Modification and Optimization of MDAB Ratio to Clay. Figure 4 shows the typical FTIR spectra of Na^+-MMT before and after the modification with cationic photo-

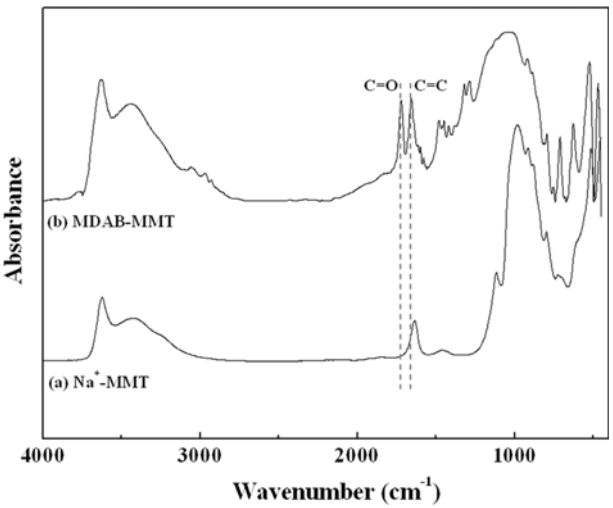

Figure 4. FTIR spectra of synthesized MDAB and the modified clay.

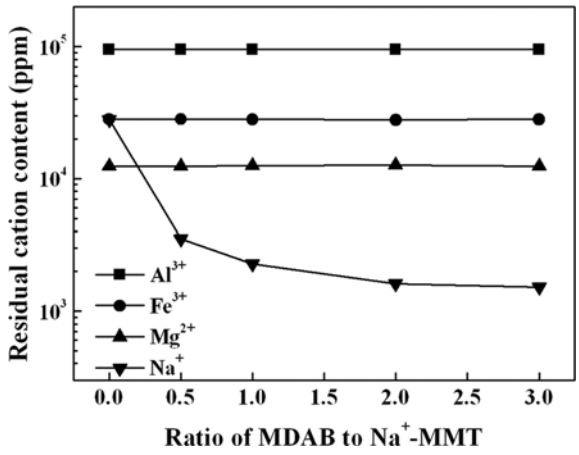

Figure 5. Residual ion contents after modification with MDAB at various MDAB/Na^+-MMT ratios.

initiator, MDAB. The modified clay showed new absorbance bands in the FTIR spectrum at 1720 and 1660 cm^{-1} for C=O and C=C stretching, respectively. These results indicated that the clays were successfully modified with MDAB by cationic exchange reaction.

In order to confirm the cation exchange reaction between MDAB and sodium ion, residual ion contents of Na^+-MMT were determined by ICP-AES. As shown in Figure 5, various cation contents were determined after treatment with MDAB. Sodium ion content was reduced with MDAB content increase while the other ion contents such as aluminum, iron and magnesium were not changed, which means only sodium ions in Na^+-MMT were replaced by MDAB. MDAB was saturated at MDAB/MMT content of 2:1, and no more reduction was observed beyond it.

XRD results after modification with MDAB with different MDAB/ Na^+-MMT ratio were shown in Figure 6. When Na^+-

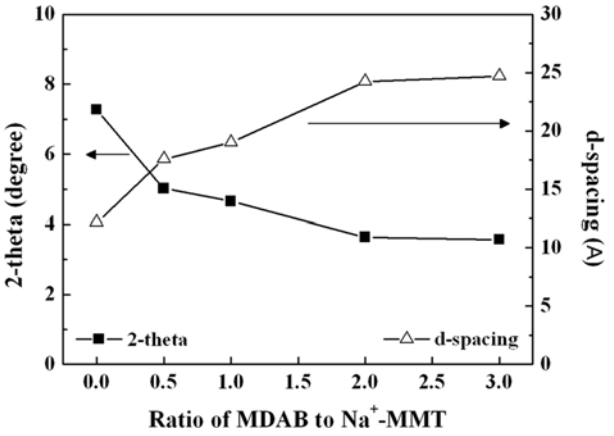

Figure 6. XRD results after modification with MDAB at various MDAB/Na^+-MMT ratios.

MMT were modified by MDAB, 2θ values were shifted toward lower angle and interlayer spacing were increased. Interlayer spacing of the modified clay was increased with relative amount of MDAB and no more increase was observed beyond the saturation point at MDAB/MMT content of 2:1 as mentioned in Figure 5. Therefore, MDAB/MMT content was optimized at 2:1.

Polymer/Nanocomposite Layer Formation. MDAB-modified clay was dispersed in 30 mL of DMF and mechanically stirred at 60 °C for 1 h under nitrogen atmosphere, and then treated by probe-type ultra-sonicator for 10 min to enhance the dispersion of clay in solution. Then the solution was mixed with EpA, HDDA and TMPTA and stirred for another 8 h at 60 °C to make composites coating solution. Nanomer 1.28E, which is organically modified commercial clay, was also tested in the same manner as MDAB for comparison test.

PEN substrate was cleaned in methanol for 10 min by bath-type ultra-sonicator and dried at 80 °C. Oxygen plasma treatment was conducted on PEN surface to enhance the adhesion property between substrate and coating layer by using plasma cleaner (Plasmatic system, U.S.A.) for 10 s at 650 watt power. The polymer/nanocomposite solution was bar coated on PEN substrate at 0.7 micron of coating thickness and then UV-cured for 8 min at 1 kW by using a high pressure mercury lamp.

WVTR values of the composite layers with different MDAB content were shown in Figure 7. Each sample has uniform MDAB/MMT clay content as 5 wt%. Increase of MDAB/MMT ratio reduced WVTR values of composite layer and it also showed the optimum point at 2:1, which coincided with the results shown in Figures 5 and 6.

Intra-Gallery and Extra-Gallery Polymerization. MDAB/MMT was compared with commercial organoclay, Nanomer 1.28E. Nanomer 1.28E has the alkyl chain to enhance the compatibility with polymer. As shown in Table I, both clays were intercalated to have *d*-spacing values two times greater than that of unmodified Na^+-MMT. Both clays have

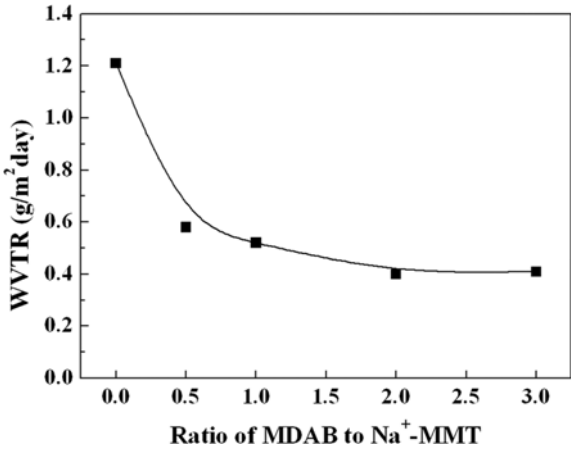

Figure 7. WVTR results of EpA/MDAB-MMT composites at various MDAB/Na^+-MMT ratios (Clay content : 5 wt%).

Table I. Change of XRD Characteristics of Clays by the Modification

	Unmodified Clay	Modified Clay	
	Na^+-MMT	Nanomer l.28E	MDAB-MMT
2-Theta (degree)	7.27	3.74	3.64
D-Spacing (Å)	12.16	23.63	24.24

quite similar 2-theta and *d*-spacing values before the photopolymerization of EpA. However, when they underwent photopolymerization of EpA, great differences were observed between two clays.

Since MDAB worked as a photoinitiator of EpA polymerization, great amount of EpA oligomer could be photopolymerized at the interlayer of clay (EpA/MDAB-MMT) as shown in Figure 3(a), which is called as intra-gallery polymerization. Therefore, more intercalation was expected to still increase the *d*-spacing. As shown in Table II, EpA/MDAB-MMT sample showed no peaks above 2.0 degree, the detection limit of the apparatus. MDAB-MMT underwent the intra-gallery polymerization to reach more intercalation, which confirmed the *d*-spacing greater than 44.56 Å corresponding to 2-theta of 2.00 degree.

As shown in Figure 3(b), limited amount of EpA oligomer could penetrate into the interlayer of Nanomer 1.28E and photopolymerization was performed between the tactoids, which is called as extra-gallery polymerization (EpA/1.28E). Slight increase of *d*-spacing was observed from 23.63 to 30.89 Å after the extra-gallery polymerization for EpA/1.28E as shown in Table II. Then we could conclude that intra-gallery polymerization for EpA/MDAB-MMT attained more intercalation than extra-gallery intercalation for EpA/1.28E and even exfoliation was expected for EpA/MDAB-MMT sample.

Table II shows the WVTR results of bare PEN substrate and composites layers of EpA/MDAB-MMT and EpA/1.28E. Barrier property of PEN substrate was enhanced for both cases when compared with that of unmodified Na^+-MMT (EpA/MMT) due to the compatibility enhancement with polymer matrix. Nanocomposite of EpA/MDAB-MMT by intra-gallery polymerization showed better barrier property than EpA/1.28E composite formed by extra-gallery polymerization.

In polymer-clay nanocomposite system, degree of intercalation and exfoliation in general depends on the layer charge density, popularly known as the cation exchange capacity (CEC). Also, the CEC affect the packing geometry of cation, the degree of surface coverage and the overall interlayer distance.[16] They also reported that the higher CEC oragnoclay showed compact tactoid morphology, compared with lower CEC organoclay, due to the differences in magnitude of the attractive electrostatic forces originated from various CEC values. 1.28E has greater CEC value than MMT and smaller tactoid size, and MDAB sample is expected to enhance CEC value and to reduce the tactoid size. Therefore, the clays in EpA/MDAB-MMT composites were more intercalated than those in EpA/1.28E composites, which implied the decrease of tactoid size. Decrease of tactoid size below the wavelength of light reduced the light scattering through the sample to enhance the optical transmittance of the EpA/MDAB sample compared with that of EpA/1.28E.

Morphology Analysis by TEM. Figure 8. shows the TEM images of various samples of polymer/nanocomposite; (a) EpA/MMT, (b) EpA/1.28E, and (c) EpA/MDAB-MMT. TEM images at low magnification revealed that clay was not well dispersed in polymer matrix for every sample in Figure 8. Paul *et al*. demonstrated that completely dispersed and exfoliated nanocomposites were prepared by twin screw extruder under very high shear force.[17,18] In this work the samples were prepared by solution mixing at low shear force, and we could not expect such complete dispersion and exfoliation.

Table II. Characteristics of EpA/Nanocomposites for Various Clays (Clay content : 5 wt%)

		EpA/Unmodified Nanocomposites	EpA/Modified Nanocomposites	
	Bare PEN	EpA/MMT	EpA/l.28E	EpA/MDAB-MMT
2-Theta (degree)	-	4.62	2.86	< 2.0
D-Spacing (Å)	-	19.11	30.89	> 44.56
WVTR (g/m²day)	1.42	1.21	0.7	0.39
Transmittance (%)	88.1	76.3	80.6	83.2

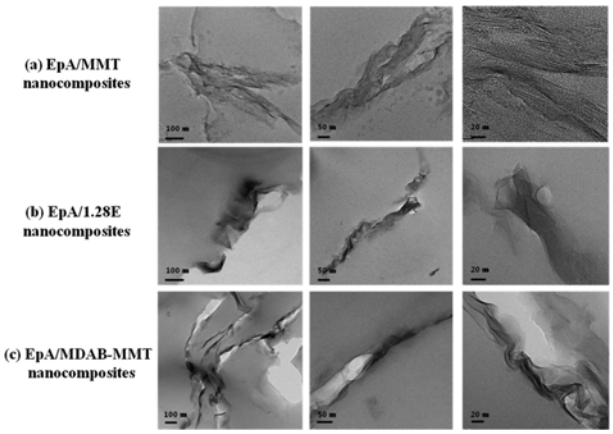

Figure 8. Cross-sectional TEM images of various EpA/nanocomposites (Clay content : 5 wt%).

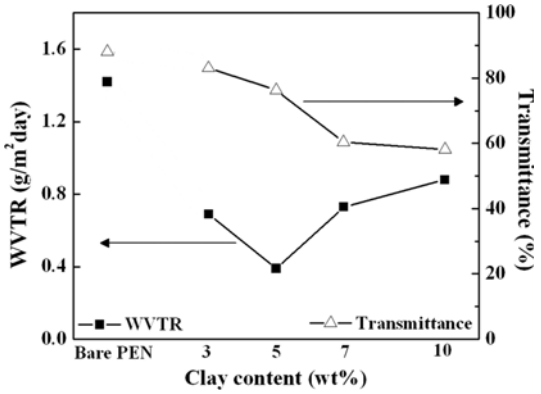

Figure 9. WVTR and Transmittance variations of EpA/MDAB-MMT nanocomposite with various clay contents (MDAB:Na^+-MMT=2:1).

However, we could observe the decrease of tactoid thickness in Figure 8 as we modified the nanoclay from MMT (a), to 1.28E (b) and to MDAB-MMT (c). Intra-gallery polymerized sample (c) had thinner tactoid than extra-gallery polymerized sample (b) and unmodified sample (a). What we could observe is that intra-gallery polymerized sample achieved better dispersion than the others, even though clay dispersion was not as good as that of twin screw sample. We also confirmed that *d*-spacing was more increased by intra-gallery polymerization and that the samples were more intercalated. We confirmed that 2 theta value exceeded the detection limit, and d-spacing increased greater than 44.56 Å.

Optimization of Clay Contents. Effects of clay content on WVTR and light transmittance were examined for EpA/MDAB-MMT samples. As shown in Figure 9, WVTR decreased with increasing clay loading until critical content (5 wt%) and then increased with increasing clay content due to the agglomeration of clays. Optical transmittance was gradually decreased with clay content as expected. However, serious optical transmittance decay was observed beyond 5 wt% of clay content due to the clay aggregation. It was also confirmed from the TEM results as shown in Figure 10 that the clay was more aggregated above the critical content (5 wt%). The clay content was optimized at 5 wt% for barrier layer on PEN substrate with less degradation of optical property.

Final morphology of coating layer was shown in Figure 11. EpA/MDAB-MMT composites by using 5% of clay showed the best clay dispersion and exfoliation. MDAB modified clay, which has methacrylate functional group, was homogeneously dispersed in the polymer matrix due to good compatibility. At a high magnification, each platelet of clay showed exfoliated structures. These results confirmed that intra-gallery polymerization induced clay dispersion and exfoliation.

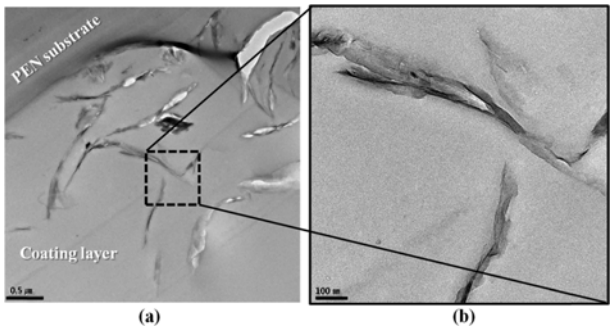

Figure 11. Final morphology of EpA/MDAB-MMT nanocomposites: (a) low magnification and (b) high magnification (MDAB:Na^+-MMT =2:1, Clay content : 5 wt%).

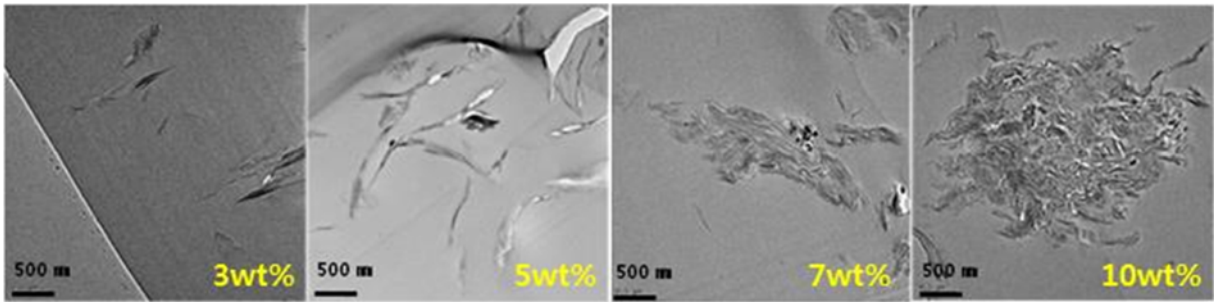

Figure 10. Cross-sectional TEM images of EpA/MDAB-MMT nanocomposite with various clay contents. (MDAB:Na^+-MMT=2:1).

Conclusions

Polymer/nanocomposite coating layers were successfully formed on plastic substrates for flexible display. MDAB, which is a photo-initiator as well as an intercalating agent, was successfully synthesized. Na^+-MMT was modified with MDAB to induce the intra-gallery polymerization and to increase *d*-spacing. Intra-gallery polymerization was better than extra-gallery polymerization to decrease WVTR because of inducing photo-initiation at the interlayer of clay. Polymer/clay nanocomposite layers enhanced the barrier property of substrate while maintaining the optical properties.

Acknowledgments. This research was supported by a grant from the Fundamental R&D Program for Technology of World Premier Materials (WPM) and RIC-CAMID of Kyung Hee University.

References

(1) Z. Hongli, X. Zhengguo, L. Detao, L. Yuanyuan, J. N. Weadock, F. Zhiqiang, H. Jinsong, and H. Liangbing, *Energy Environ. Sci.,* **6**, 2105 (2013).
(2) S. Hideharu, S. Kaoru, M. Takeshi, and S. Yukihiro, *Japanese J. Appl. Phys.*, **51**, 05EB02 (2012).
(3) Y. Kojima, A. Usuki, M. Kawasumi, A. Okada, Fukushima, T. Kurauchi, and O. Kamigaito, *J. Mater. Res.*, **8**, 1185 (1993).
(4) G. Choudalakis and A. D. Gotsis, *Eur. Polym. J.*, **45**, 967 (2009).
(5) E. P. Giannelis, R. Krishnamorti, and E. Manias, *Adv. Polym. Sci.*, **138**, 107 (1999).
(6) E. P. Giannelis, *Adv. Mater.*, **8**, 29 (1996).
(7) H. Miyuki, M. Takeharu, and O. Mitsukazu, *J. Polym. Sci. Part B: Polym. Phys.*, **47**, 1753 (2009).
(8) A. Leszczynska, J. Njuguna, K. Pielichowski, and J. R. Banerjee, *Thermochim. Acta*, **454**, 1 (2007).
(9) Y. Mostafa, M. Tahereh, C. Nathalie, and H. Pascal, *Compos. Sci. Technol.*, **82**, 47 (2013).
(10) K. Zahouily, C. Decker, S. Benfarhi, and J. Baron, *J. Proc. Rad. Tech. North Am.*, 309 (2002).
(11) S. Subramani, S. W. Choi, J. Y. Lee, and J. H. Kim, *Polymer*, **48**, 4691 (2007).
(12) P. E. Burrows, G. L. Graff, M. E. Gross, P. M. Martin, M. Hall, E. Mast, C. Bonham, W. Bennett, L. Michalski, M. Weaver, J. J. Brown, D. Fogarty, and L. S. Sapochak, *Proc. SPIE*, **4105**, 75 (2001).
(13) O. Akane and U. Arimitsu, *Macromol. Mater. Eng.*, **291**, 1449 (2006).
(14) Z. Hua, Z. Yong, P. Zonglin, and Z. Yinxi, *Polym. Test.*, **23**, 217 (2004).
(15) Z. Yangling, X. Weijian, L. Guangpeng, Q. Deyue, and S. Shengpei, *J. Appl. Polym. Sci.*, **111**, 813 (2009).
(16) L. M. Stadtmueller, K. R. Ratinac, and S. P. Ringer, *Polymer*, **46**, 9574 (2005).
(17) J. W. Cho and D. R. Paul, *Polymer*, **42**, 1083 (2001).
(18) T. D. Fornes, P. J. Yoon, D. L. Hunter, H. Keskkula, and D. R. Pau, *Polymer*, **43**, 5915 (2002).